Poly(ADP-ribose) engages the TDP-43 nuclear-localization sequence to regulate granulo-filamentous aggregation

Leeanne McGurk[1#], Edward Gomes[2#], Lin Guo[2#], James Shorter[2*], and Nancy M. Bonini[1*].

Affiliations
[1]Department of Biology, University of Pennsylvania, Philadelphia, PA 19104, USA
[2]Department of Biochemistry and Biophysics, Perelman School of Medicine, University of Pennsylvania, Philadelphia, PA 19104, USA

[#]co-first authors
***co-corresponding authors.**

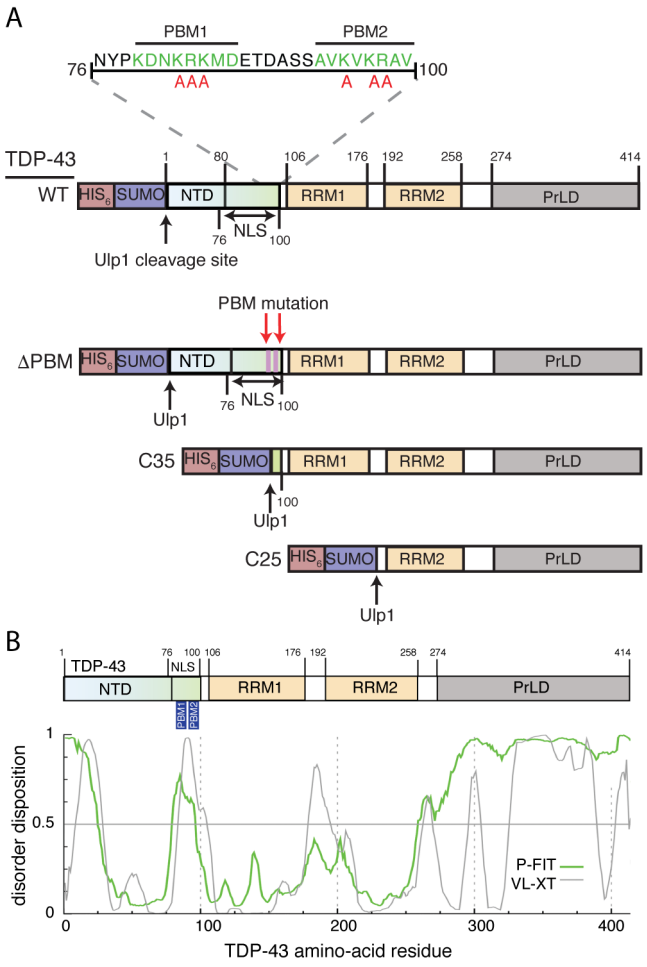

Figure S1. TDP-43 domain architecture.

A. Schematic of TDP-43 constructs used in this study. The Ulp1 cleavage site is downstream of the HIS_6-SUMO-tag and upstream of the TDP-43 ATG-start codon in all constructs. The amino acids in green are the PAR-binding motifs (PBM1 and PBM2), and the red amino acids represent the mutations made to generate TDP-43-ΔPBM. NTD: N-terminal domain. NLS: Nuclear localization sequence. PBM: PAR-binding motif. RRM: RNA recognition motif. PrLD: prion-like domain.

B. Schematic of the domain architecture of TDP-43 and predicted disorder. Disorder was predicted using an online database with the VL-XT and P-Fit (PONDR-Fit) algorithms. [1-3]

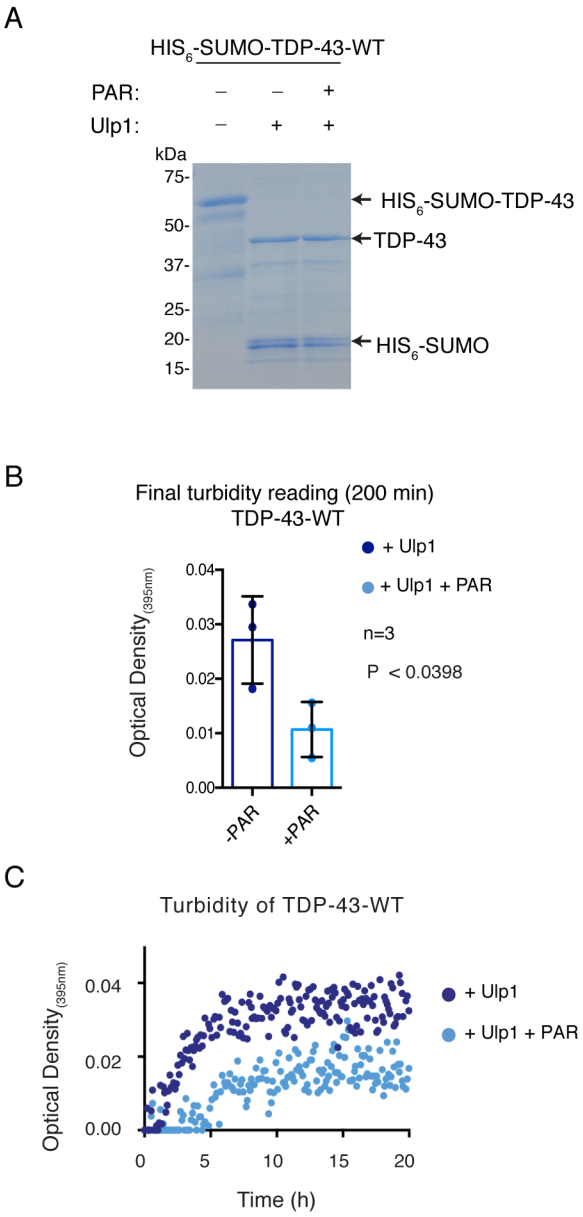

Figure S2: PAR reduces TDP-43 aggregation *in vitro*.

A. Incubation of Ulp1 with purified 10 μM SUMO-TDP-43-WT results in cleavage of the N-terminal HIS_6-SUMO-tag to produce TDP-43-WT and HIS_6-SUMO at the expected molecular weights. PAR at substoichiometric amounts (6 μM equivalents to mono(ADP-ribose)) had no effect on Ulp1-cleavage of 10 μM HIS_6-SUMO-TDP-43-WT. The final turbidity samples (200 min) were processed for SDS-PAGE and visualized by Coomassie blue staining.

B. PAR, at a concentration of 6 μM equivalents to mono(ADP-ribose), reduces the final optical density measurement at 395 nm (200 min) of 10 μM TDP-43-WT compared to PAR buffer control. The mean of the final OD_{395} (± SD) is presented. The n value is 3 independent experiments performed on two separate preparations of protein and demonstrates the reproducibility of the data. A two-tailed and unpaired T-test was performed.

C. Ulp1-cleavage of 10 μM His_6-SUMO-TDP-43-WT at 30^{o}C leads to an increase in optical density at 395 nm that plateaus after 10-20 h. Co-incubation with PAR at 6 μM equivalents to mono(ADP-ribose) reduces the amplitude of the plateau phase, indicating that PAR reduces TDP-43 aggregation. Graph is a representative dataset.

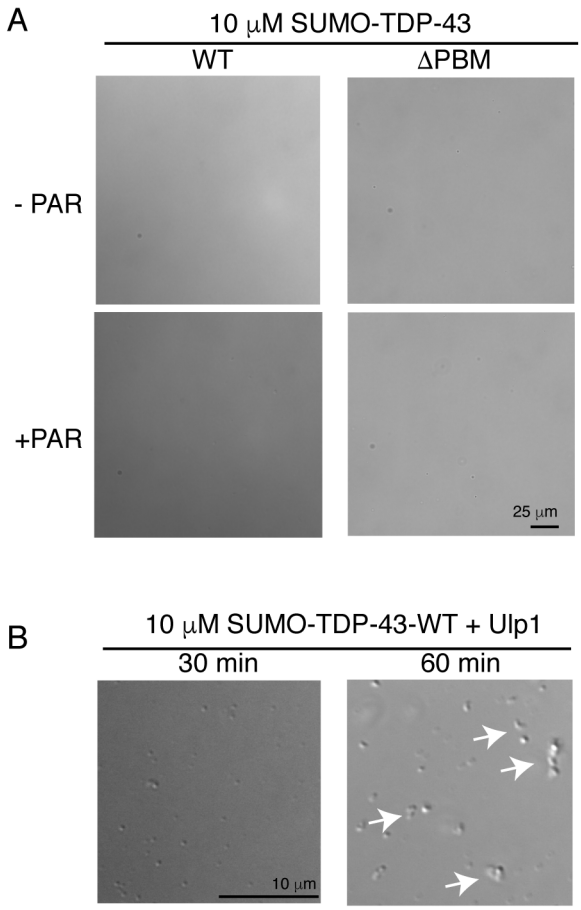

Figure S3. **Examination of cleaved TDP-43 by optical microscopy.**

A. SUMO-TDP-43-WT and SUMO-TDP-43-ΔPBM in 70 mM NaCl remained diffuse as examined by differential interference contrast (DIC) microscopy.

B. Ulp1-cleaved SUMO-TDP-43-WT in 70mM NaCl forms spherical structures that after 60 min coalesce into irregular solid structures (arrows).

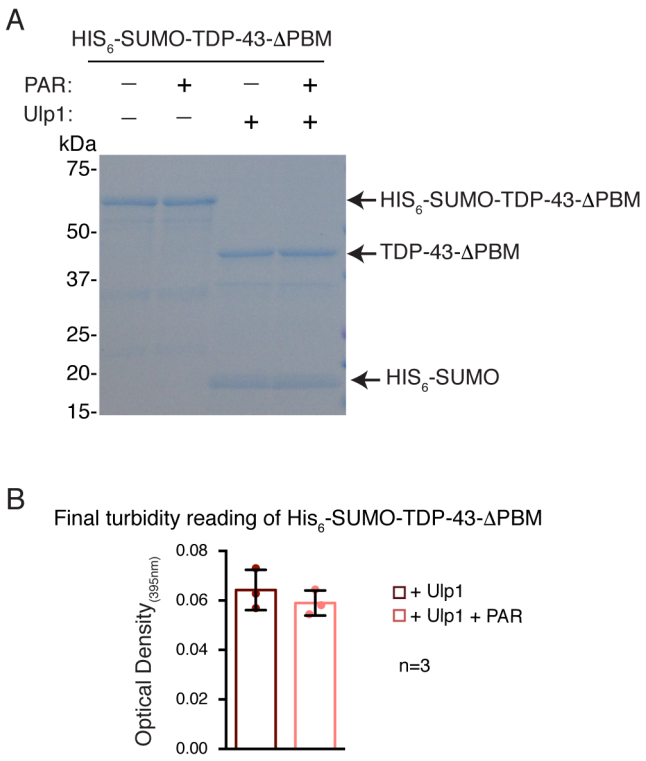

Figure S4. **The PAR-binding motifs are required for PAR-mediated inhibition of TDP-43 aggregation.**

A. Incubation of Ulp1 with purified HIS_6-SUMO-TDP-43-ΔPBM (10 µM) results in cleavage of the N-terminal HIS_6-SUMO tag to produce TDP-43-ΔPBM and HIS_6-SUMO at the expected molecular weights. PAR at 6 µM equivalents to mono(ADP-ribose) has no effect on Ulp1-cleavage of HIS_6-SUMO-TDP-43-ΔPBM (10 µM). The final turbidity protein samples were processed for SDS-PAGE and visualized by Coomassie blue staining.

B. The final optical density measurement at 395 nm (54 h) of 10 µM SUMO-TDP-43-ΔPBM is unaltered by the addition of PAR at a concentration of 6 µM equivalents to mono(ADP-ribose). The mean of the final optical density reading at 395 nm (± SD.) from 3 independent experiments from 2 independent protein preparations is presented and demonstrates the reproducibility of the data. A two-tailed unpaired T-test was performed. The final turbidity readings were not significantly different ($P = 0.3952$).

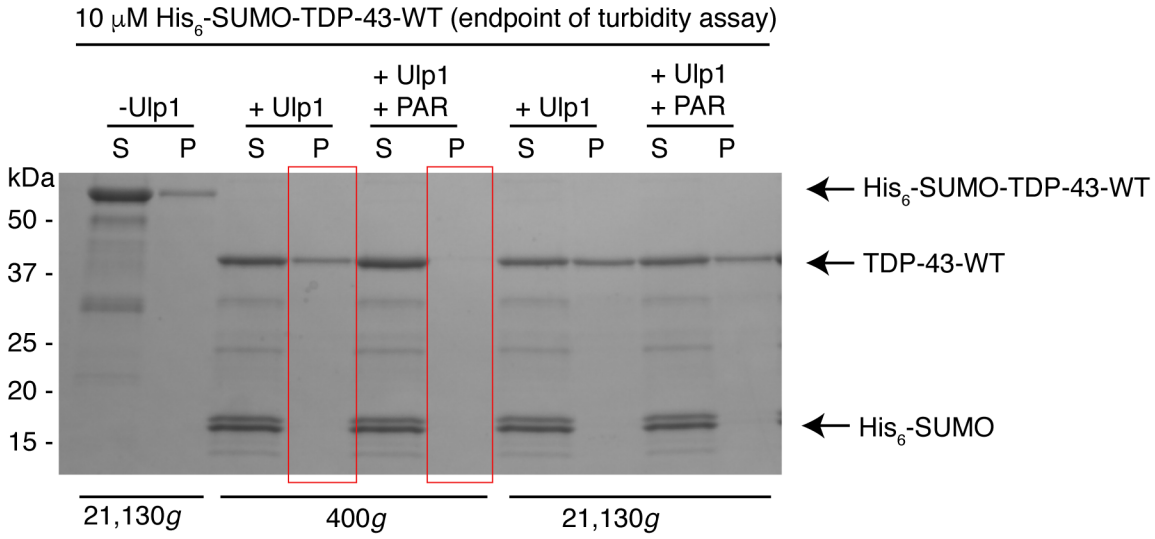

Figure S5. PAR inhibits formation of large TDP-43 aggregates.

HIS_6-SUMO-TDP-43-WT was subjected to a turbidity assay and the resulting protein was separated into the supernatant (S) and the pellet fraction (P), the protein samples were denatured and electrophoresed on an SDS-polyacrylamide gel. At 400*g*, only the large aggregates are pelleted, and in the presence of 6 μM PAR the amount the TDP-43-WT in the pellet fraction (P) was reduced (compare red boxes), see Figure 3B for quantification. At 21,130*g*, large and small TDP-43 aggregates are pelleted and the presence of PAR had no effect on the amount of TDP-43-WT in the insoluble pellet. For quantification see Figure 3C. Consistent with the TEM analysis (see Figure 3A-B), these data indicate that PAR inhibits the formation of large TDP-43 aggregates.

A

	1 μM HIS_6-SUMO-TDP-43			α-Syn	
	WT+Ulp1	C25 -Ulp1	C25 +Ulp1	(1 μM)	Buffer
ThT fluorescence (AU)	297	296	204	2479	261

B

	10 μM HIS_6-SUMO-TDP-43			α-Syn	
	WT+Ulp1	C25 -Ulp1	C25 +Ulp1	(1.8 μM)	Buffer
ThT fluorescence (AU)	676	277	683	3640	207

Figure S6. TDP-43-C25 aggregates were not reactive to Thioflavin T.

A. TDP-43-WT and TDP-43-C25 (both 1 μM) at the endpoint of a turbidity assay were tested for reactivity to 10 μM Thioflavin T (ThT) excited at 440 nm. Emission was collected at 482 nm. While the positive control, α-Synuclein (α-Syn) fibrils, was reactive to ThT, TDP-43-WT, HIS_6-SUMO-TDP-43-C25 and TDP-43-C25 were no different to the buffer alone negative control. These data indicate that under these conditions these protein variants do not have amyloid-like properties.

B. At higher protein concentrations, TDP-43-WT, HIS_6-SUMO-TDP-43-C25 and TDP-43-C25 remained non-reactive to ThT.

METHODS

Plasmids

Human TDP-43 (Uniprot IDL: Q13148), TDP-43-ΔPBM, TDP-43-C35 and TDP-43-C25 subcloned into pE-SUMO (LifeSensors, Malvern, PA) are as described. [4] Ulp1 was cloned into pFGET19 (Addgene #64697). All plasmid inserts were fully sequenced and confirmed to be correct.

PAR polymer

Free PAR (commercially obtained from TREVIGEN (Gaithersburg, MD)) was synthesized from PARP-1 and ranged in size from 2-300 ADP-ribose subunits. Molar equivalencies were calculated by TREVIGEN. Briefly, the Absorbance of the PAR at 258 nm was divided by the extinction coefficient of ADP-ribose (13, 500 cm^{-1} M^{-1}). [5, 6]

Purification of Recombinant His_6-SUMO-TDP-43 and aggregation assays

HIS_6-SUMO N-terminally tagged TDP-43-WT, TDP-43-ΔPBM, TDP-43-C35 and TDP-43-C25 were purified as described. [4] Yeast HIS_6-Ulp1 protease (Ulp1, Uniprot ID: Q02724) was purified as described for His_6-SUMO N-terminally tagged TDP-43-WT. [4] Prior to the turbidity assay, protein was thawed and centrifuged at 16,100*g* for 10 min to remove any preformed aggregates. Protein concentration was determined by Bradford assay (Bio-Rad, Hercules, CA). The kinetics of TDP-43 aggregation were assessed via turbidity assay by measuring the optical density at 395 nm at regular time intervals. Briefly, 10 µM of the indicated protein was incubated in 50 mM HEPES-NaOH (pH 7.5), 5% glycerol, 70 mM NaCl, 5 mM DTT, 6 mM TrisHCl (pH 8), 0.6 mM EDTA with shaking at 30°C in Nunc 96-well optical bottom plates (Thermo Fisher Scientific, Waltham, MA) with PAR (Trevigen, Gaithersburg, MD) at a concentration of 6 µM mono(ADP-ribose) equivalents in 10 mM Tris-HCl (pH 8) and 1 mM EDTA, or equivalent volume of buffer (10 mM Tris-HCl [pH 8] and 1 mM EDTA). At time 0, cleavage of the HIS_6-SUMO tag was initiated with 1.8 µg of Ulp1. Turbidity data are represented as the relative change, which was calculated by subtracting the initial OD_{395} value from the final OD_{395} value.

Transmission electron microscopy

Transmission electron microscopy (TEM) of the aggregates was performed as described. [7] Briefly, at the end point of the turbidity assay (200 min for TDP-43-WT and 54 h for TDP-43-ΔPBM) samples were diluted two-fold, 10 μL of the diluted sample was adsorbed onto 300-mesh Formvar/carbon-coated copper grids (Electron Microscopy Sciences, Hatfield, PA) and stained with 2% (w/v) uranyl acetate. Excess uranyl acetate solution was removed and the grids were dried. Samples were imaged using a FEI-Tecnai and a JEOL-1010T12 transmission electron microscope. For quantification, 2-3 micrographs representing each protein were analyzed by ImageJ. [8] 1534-5829 aggregates were quantified for each protein condition.

Sedimentation assay

HIS_6-SUMO-TDP-43-WT (10 μM) was subjected to a turbidity assay and at the end of the 200-min reaction, the resulting protein was separated into the supernatant fraction (S) and the pellet fraction (P) by centrifugation for 10 min at 4°C with speed of 400*g* or 21,130*g*. Supernatant and pellet fractions were then denatured in Laemmli buffer and β-mercaptoethanol, heat denatured at 99°C. 11.4% of supernatant or pellet fraction was loaded and protein was resolved by sodium dodecyl sulfate polyacrylamide gel electrophoresis (SDS–PAGE) and stained with Coomassie Brilliant Blue, and the amount in either fraction (% total) was determined by densitometry in comparison to known quantities of the SUMO-TDP-43-WT. Under these conditions, in the presence of Ulp1 and the absence of PAR, ~50% of the TDP-43 remained in the supernatant fraction at both centrifugal speeds (Figure 3C).

Thioflavin T assay

HIS_6-SUMO-TDP-43-WT and HIS_6-SUMO-TDP-43-C25 (10 μM) was aggregated *in vitro* as above. At the end of the 200-min reaction, protein was assessed without dilution or with dilution to 1 μM using reaction buffer (50mM HEPES-NaOH (pH 7.5), 5% glycerol, 70 mM NaCl, 5 mM DTT, 6 mM TrisHCl (pH 8), 0.6 mM EDTA). Thioflavin-T (ThT) was added into the reaction at 10 μM and sample was excited at 440 nm with a 5 nm bandwidth. Fluorescence signal was collected at 482 nm with a 10 nm bandwidth. α-Synuclein fibrils assembled as described[9] in reaction buffer were used as a positive control.

Statistics

All statistics were carried out using Graphpad prism 6 software.

REFERENCES

[1] Li, X., Romero, P., Rani, M., Dunker, A. K., and Obradovic, Z. (1999) Predicting Protein Disorder for N-, C-, and Internal Regions, *Genome Inform Ser Workshop Genome Inform 10*, 30-40.

[2] Romero, P., Obradovic, Z., Li, X., Garner, E. C., Brown, C. J., and Dunker, A. K. (2001) Sequence complexity of disordered protein, *Proteins 42*, 38-48.

[3] Xue, B., Dunbrack, R. L., Williams, R. W., Dunker, A. K., and Uversky, V. N. (2010) PONDR-FIT: a meta-predictor of intrinsically disordered amino acids, *Biochim Biophys Acta 1804*, 996-1010.

[4] McGurk, L., Gomes, E., Guo, L., Mojsilovic-Petrovic, J., Tran, V., Kalb, R. G., Shorter, J., and Bonini, N. M. (2018) Poly(ADP-Ribose) Prevents Pathological Phase Separation of TDP-43 by Promoting Liquid Demixing and Stress Granule Localization, *Molecular cell 71*, 703-717 e709.

[5] Schultheisz, H. L., Szymczyna, B. R., and Williamson, J. R. (2009) Enzymatic synthesis and structural characterization of 13C, 15N-poly(ADP-ribose), *J Am Chem Soc 131*, 14571-14578.

[6] Shah, G. M., Poirier, D., Duchaine, C., Brochu, G., Desnoyers, S., Lagueux, J., Verreault, A., Hoflack, J. C., Kirkland, J. B., and Poirier, G. G. (1995) Methods for biochemical study of poly(ADP-ribose) metabolism in vitro and in vivo, *Anal Biochem 227*, 1-13.

[7] Johnson, B. S., Snead, D., Lee, J. J., McCaffery, J. M., Shorter, J., and Gitler, A. D. (2009) TDP-43 is intrinsically aggregation-prone, and amyotrophic lateral sclerosis-linked mutations accelerate aggregation and increase toxicity, *The Journal of biological chemistry 284*, 20329-20339.

[8] Rueden, C. T., Schindelin, J., Hiner, M. C., DeZonia, B. E., Walter, A. E., Arena, E. T., and Eliceiri, K. W. (2017) ImageJ2: ImageJ for the next generation of scientific image data, *BMC Bioinformatics 18*, 529.

[9] Luk, K. C., Covell, D. J., Kehm, V. M., Zhang, B., Song, I. Y., Byrne, M. D., Pitkin, R. M., Decker, S. C., Trojanowski, J. Q., and Lee, V. M. (2016) Molecular and Biological Compatibility with Host Alpha-Synuclein Influences Fibril Pathogenicity, *Cell Rep 16*, 3373-3387.